A quantitative method to determine the optimal stress field for 2D 8-node quadrilateral hybrid finite element

*Canhui Zhang, Pei Liu, and Dongdong Wang

Department of Civil Engineering, Xiamen University, Xiamen, Fujian 361005, China

*Corresponding author: chzhang@xmu.edu.cn

Abstract

A quantitative method is developed to determine the optimal stress field for 2D 8-node quadrilateral hybrid stress element (HQ8). It provides a straightforward way as to that how and why the resulting element can improve its displacement response. A new inner product with material weighting matrix is defined to reveal the relationship in quantity of exact similarity degrees between different stress modes. It is different from the conventional energy product which can only qualitatively determine the orthogonality of stress and strain modes because they are considered as mathematical vectors without physical meaning. The proposed strategy includes two steps. Firstly, the basic stress modes are divided into a set of sub-modes. Secondly, the sub-mode with largest similarity degree with the basic mode is selected as the optimal assumed stress mode for a hybrid element. The optimal stress modes for HQ8 are determined when Poison's ratio is larger than 1/9 which is the case for most materials.

Keywords: 8-node quadrilateral hybrid stress element; quantitative method; optimal assumed stress field; material weighting matrix based inner product; largest similarity degree

Introduction

Since the displacement elements exhibit over rigidity, the hybrid stress element was first formulated by Pian (1964) to resolve this issue where the stress field was assumed independently as

$$\boldsymbol{\sigma} = \sum_{i=1}^{M} \boldsymbol{\sigma}_i \beta_i = \boldsymbol{P\beta} \tag{1}$$

in which $\boldsymbol{\sigma}_i$'s are the assumed stress modes, β_i's the corresponding stress parameters, and $\boldsymbol{P} = \{\boldsymbol{\sigma}_1, \cdots, \boldsymbol{\sigma}_M\}$ the stress matrix. Besides, the displacement field is assumed as $\boldsymbol{u} = \boldsymbol{Na}$, where $\boldsymbol{N}$ is the shape function matrix and $\boldsymbol{a}$ the nodal displacement vector of the element. Then the element strain can be expressed as $\boldsymbol{\varepsilon} = \boldsymbol{Du} = \boldsymbol{Ba}$ where $\boldsymbol{B} = \boldsymbol{DN}$ is the geometry matrix in which $\boldsymbol{D}$ is the matrix of differential operator. Thus the element stiffness matrix can be obtained via the Hellinger-Reissner variational principle as follows

$$\boldsymbol{K} = \boldsymbol{G}^T \boldsymbol{H}^{-1} \boldsymbol{G} \tag{2}$$

where

$$\boldsymbol{H} = \int_{V^e} \boldsymbol{P}^T \boldsymbol{SP} dV, \ \boldsymbol{G} = \int_{V^e} \boldsymbol{P}^T \boldsymbol{B} dV \tag{3}$$

Besides, the following relationships between the stress parameters and nodal displacements can also be obtained as

$$\boldsymbol{\beta} = \boldsymbol{H}^{-1} \boldsymbol{Ga} \tag{4}$$

In the hybrid finite element analysis, a stress subspace including all the assumed stress modes was introduced by Zhang, Feng and Huang (2002) as

$$\mathscr{S}_i = \left\{ \boldsymbol{\sigma} \in (L^2(V^e))^{n_d} \ \middle| \ \boldsymbol{\sigma} = \sum_{k=1}^{i} \beta_k \boldsymbol{\sigma}_k, \ \beta_k \in \mathbb{R} \right\} \in \mathbb{R}^{n_d}, \ i = 1, 2, \cdots, M \tag{5}$$

where n_d is the dimension of $\mathscr{S}$, i.e., $n_d = 3$ for 2D and $n_d = 6$ for 3D. To develop high performance hybrid stress elements, a number of approaches for obtaining the satisfactory stress modes have been presented such as Pian and Sumihara (1984), Han and Hoa (1993), Sze (1996), Wu and Cheung (1995). The concept of natural deformation modes for hybrid elements was introduced by Huang (1991). Unfortunately since these natural deformation modes are very complicated, an iterative numerical procedure has to be employed to find the relating natural stress modes. Pian and Chen (1983) presented the basic deformation modes to determine the necessary stress modes, but the shear components were ignored in their basic strains. Moreover, because the energy product is used, their method is limited to the qualitative analysis between the basic strain modes and the stress modes. Zhang and Wang (2006, 2010) proposed a selection method with basic deformation modes to improve the classification method by Feng et al. (1997). The complicated natural deformation modes are replaced by the simple basic deformation modes and the energy product was used to avoid the numerical modal analysis. Zhang et al. (2011) developed the basic deformation modes into the orthogonal basic deformation modes. Zhang et al. (2006) compared the performance of different elements with different assumed stress fields. For higher-order elements, Bilotta and Casciaro (2002) proposed a 2D 8-node hybrid element with 14 modes in his assumed stress field so the number of modes is larger than the least for the optimal requirement of 13 modes. Cen et al. (2011) proposed the stress functions to derive the assumed stress for hybrid-stress function plane element with high accuracy.

However, one existing problem is that there is still lack of rational way to find the satisfactory stress modes and tell that whether or not they are optimal for hybrid stress elements, particularly for those of higher-order. It is our attempt to find a suitable method to reveal the quantitative relationship between the different stress modes and obtain the optimal assumed stress modes for 8-node quadrilateral hybrid element (HQ8).

A quantitative method to determine the optimal stress field

Basic deformation modes and their relating basic stress modes

For the hybrid element with n degrees of freedom including r rigid body motions and $m = n - r$ deformations, following the procedures by Zhang and Wang (2006, 2010) the rigid body motions and pure deformations can be determined and separated. Thus the displacement field for pure deformation can be expressed as

$$\boldsymbol{u} = \sum_{i=1}^{m} \alpha_i \boldsymbol{u}_i = \bar{\boldsymbol{N}}\boldsymbol{\alpha}, \ \bar{\boldsymbol{N}} = \{\boldsymbol{u}_1, \cdots, \boldsymbol{u}_m\}, \ \boldsymbol{\alpha} = \begin{Bmatrix} \alpha_1 \\ \vdots \\ \alpha_m \end{Bmatrix} \tag{6}$$

where α_i's are the independent coefficients and $\boldsymbol{u}_i$'s the basic displacements. The nodal displacement vectors for pure deformation can be readily obtained by substitution of the nodal coordinates into Eq. (6) as

$$\mathbf{a} = \sum_{i=1}^{m} \alpha_i \mathbf{a}_i = \mathbf{A}\boldsymbol{\alpha}, \ \mathbf{A} = \{\mathbf{a}_1, \cdots, \mathbf{a}_m\} \tag{7}$$

where $\boldsymbol{a}_i$'s are the basic deformation modes. By the geometry equation $\boldsymbol{\varepsilon} = \boldsymbol{D}\boldsymbol{u} = \boldsymbol{B}\boldsymbol{a}$ with the basic displacements in Eq. (6), the hybrid element strain can be expressed as

$$\boldsymbol{\varepsilon} = \sum_{i=1}^{m} \alpha_i \boldsymbol{\varepsilon}_i = \bar{\boldsymbol{B}}\boldsymbol{\alpha}, \ \bar{\boldsymbol{B}} = \boldsymbol{D}\bar{\boldsymbol{N}} = \{\boldsymbol{\varepsilon}_1, \cdots, \boldsymbol{\varepsilon}_m\}, \ \boldsymbol{\varepsilon}_i = \boldsymbol{B}\boldsymbol{a}_i \tag{8}$$

where $\boldsymbol{\varepsilon}_i$'s are the basic strain modes corresponding to the basic deformation modes. Because the basic deformation modes include all the m possibilities of the element to deform, they indeed can be used to describe any deformation of the element within these possibilities. In addition, since they are unique because of their linear independence, the derived basic strain modes were used to determine the zero-energy deformation modes in the element by Pian and Chen (1983) as well as Zhang and Wang (2006, 2010). However, in this paper we use the basic stress modes derived from

the basic strain modes to find the optimal stress modes for hybrid stress element. From Eq. (8) the following stress field can be expressed as

$$\boldsymbol{\sigma}' = \boldsymbol{C}\boldsymbol{\varepsilon} = \sum_{i=1}^{m} \alpha_i \boldsymbol{\sigma}_i' = \boldsymbol{P}'\boldsymbol{\alpha} = \boldsymbol{CBA}, \ \boldsymbol{P}' = \{\boldsymbol{\sigma}_1', \cdots, \boldsymbol{\sigma}_m'\} \tag{9}$$

where $\boldsymbol{\sigma}_i' = \boldsymbol{C}\boldsymbol{\varepsilon}_i = \boldsymbol{CBa}_i$ are the basic stress modes. In fact the stress field in Eq. (9) is that for the displacement element corresponding to the hybrid stress element. In other words, the stress field for the displacement counterpart can be expressed using the basic stress modes. That is because the basic deformation modes are derived directly from the displacement field (Zhang and Wang, 2006, 2010). As we know, the number of assumed stress modes for hybrid element should satisfy $M \geq m = n - r$. Because the number of the basic stress modes is equal to the degrees of freedom for element $m = n - r$, it is the least for the optimal requirement. However, inside the basic stress modes, some components are unnecessary. To verify this, we can take the basic stress modes as the assumed stress modes for hybrid element as $\boldsymbol{\sigma}_i = \boldsymbol{\sigma}_i'$, $i = 1, 2, \cdots, m$, namely, the stress field for hybrid element is assumed as $\boldsymbol{\sigma} = \boldsymbol{P}'\boldsymbol{\beta}'$. Noting that $\boldsymbol{S} = \boldsymbol{C}^{-1}$, by Eq. (9) one has

$$\boldsymbol{H}' = \int_{V^e} \boldsymbol{P}'^T \boldsymbol{S} \boldsymbol{P}' dV = \boldsymbol{A}^T \boldsymbol{K}' \boldsymbol{A}, \ \boldsymbol{G}' = \int_{V^e} \boldsymbol{P}'^T \boldsymbol{B} dV = \boldsymbol{A}^T \int_{V^e} \boldsymbol{B}^T \boldsymbol{CB} dV = \boldsymbol{A}^T \boldsymbol{K}' \tag{10}$$

where $\boldsymbol{K}'$ is the stiffness matrix for the displacement counterpart as

$$\boldsymbol{K}' = \int_{V^e} \boldsymbol{B}^T \boldsymbol{CB} dV \tag{11}$$

Equation (10) indicates that $\boldsymbol{H}'$ represents the energies of the displacement counterpart corresponding to the basic deformation modes. Substituting Eqs. (10) into Eq. (4), the stress parameters for hybrid element can be calculated as

$$\boldsymbol{\beta}' = \boldsymbol{H}'^{-1} \boldsymbol{G}' \boldsymbol{a} = (\boldsymbol{A}^T \boldsymbol{K}' \boldsymbol{A})^{-1} (\boldsymbol{A}^T \boldsymbol{K}') \boldsymbol{A}\boldsymbol{\alpha} = \boldsymbol{\alpha} \tag{12}$$

It is found that the stress parameters are exactly equal to the independent parameters for basic stress modes. So, consider Eq. (9), the stress field for hybrid element can be derived by Eq. (1) with Eq. (12) as

$$\boldsymbol{\sigma} = \boldsymbol{P}'\boldsymbol{\beta}' = \boldsymbol{P}'\boldsymbol{\alpha} = \boldsymbol{\sigma}' \tag{13}$$

It is exactly equal to its displacement counterpart. This implies that the resulting hybrid element cannot remove the over rigidity from its displacement counterpart. In other words, there are unnecessary components inside the basic stress modes even though the number of these modes is the least as required.

Construction of optimal stress field for hybrid element

On one hand, the shortcoming of over rigidity for displacement element implies that there are unnecessary factors coupled with the necessary factors inside its stress field, i.e., the basic stress field in Eq. (9). On the other hand, there is no denying that it has great success. Therefore, the necessary factors in the basic stress field are major while the unnecessary factors are minor. Since the basic stress field can be expressed by the basic stress modes, one can conclude that there are unnecessary components coupled with the necessary components in the basic stress modes, where the necessary components are major while the unnecessary components are minor. Our attempt is to obtain the necessary components and without the unnecessary components from the basic stress modes. For this purpose our procedure consists of two steps.

Step 1 (Breaking basic stress modes into sub-modes)

We take every component of the basic stress mode to construct a sub-mode. Thus the basic stress mode is broken into several sub-modes and can be expressed by the sum of them as

$$\boldsymbol{\sigma}_i' = \sum_{k=1}^{3} (\boldsymbol{\sigma}_i')_k \ (i = 1, 2, \cdots, m) \tag{14}$$

3

where $(\boldsymbol{\sigma}_i')_k = \bar{\alpha}_{ik}\bar{\boldsymbol{\sigma}}_j$ are the sub-modes in which $\bar{\alpha}_{ik}$'s are the constant coefficients dependent upon the material parameters and $\bar{\boldsymbol{\sigma}}_j$'s the stress modes of uni-axial stress or pure shear stress without any constan coefficient. Since all the sub-modes are uni-axial stress or pure shear stress, they can only be essential and not redundant.

Step 2 (Comparing sub-modes with their basic stress mode)

The sub-modes are compared with their original basic stress mode. The sub-mode with larger similarity degree implies that it is more similar to the original basic stress mode than others, so it represents the main feature of this basic stress mode. Since the main features for the basic stress modes are good, the most similar sub-mode which reflects the main features can be selected as the optimal mode.

To investigate the quantitative relationship between the sub-modes with their basic stress modes, their similarity degree is needed which in general is defined as the cosine of the angle between vectors. According to the proposition by Zhang et al. (2007), the equivalent hybrid element can be resulted from the alternative assumed stress field in which an original mode is multiplied by a nonzero constant. It is easy to verify that the magnitude of this constant does not affect their angle while its sign does. In other words, the reverse direction of the sub-mode will change the cosine sign of its angle with original basic mode. For this sake, in this paper the similarity degree is defined as the absolute value of the cosine of the angle as

$$\text{Similarity degree} = |\cos\theta_{ik}| \qquad (15)$$

where θ_{ik} is the angle between $(\boldsymbol{\sigma}_i')_k$ and $\boldsymbol{\sigma}_i'$. Thus, $|\cos\theta_{ik}| = 1$ when $\theta_{ik} = 0°$ or $180°$, indicating $\bar{\boldsymbol{\sigma}}_j$ is in the same direction as $\boldsymbol{\sigma}_i'$ or in the reverse direction to $\boldsymbol{\sigma}_i'$. However, no matter which case, $\bar{\boldsymbol{\sigma}}_j$ plays the same role to result in the hybrid elements equivalent to each other. On the other hand, $|\cos\theta_{ik}| = 0$ when $\theta_{ik} = 90°$, indicating $(\boldsymbol{\sigma}_i')_k$ and $\boldsymbol{\sigma}_i'$ are orthogonal to each other so $\bar{\boldsymbol{\sigma}}_j$ cannot be used to suppress the zero-energy mode for the element.

For the subsequent development, the following subspaces are defined as

$$\mathscr{D} = \left\{ \boldsymbol{a} \in \mathbb{R}^n \,\middle|\, \boldsymbol{a} = \sum_{i=1}^{m} \alpha_i \boldsymbol{a}_i,\ \alpha_i \in \mathbb{R} \right\}, \qquad \mathscr{E} = \left\{ \boldsymbol{\varepsilon} \in (L^2(V^e))^{n_d} \,\middle|\, \boldsymbol{\varepsilon} = \boldsymbol{B}\boldsymbol{a},\ \boldsymbol{a} \in \mathscr{D} \right\}$$

$$\mathscr{S}' = \left\{ \boldsymbol{\sigma}' \in (L^2(V^e))^{n_d} \,\middle|\, \boldsymbol{\sigma}' = \boldsymbol{C}\boldsymbol{\varepsilon},\ \boldsymbol{\varepsilon} \in \mathscr{E} \right\}, \qquad \bar{\mathscr{S}} = \left\{ \bar{\boldsymbol{\sigma}} \in (L^2(V^e))^{n_d} \,\middle|\, \bar{\boldsymbol{\sigma}} = \sum_{j=1}^{\bar{M}} \bar{\beta}_j \bar{\boldsymbol{\sigma}}_j,\ \bar{\beta}_j \in \mathbb{R} \right\} \qquad (16)$$

where $\mathscr{D} \subset \mathbb{R}^n$ is the deformation subspace by the basic deformation modes $\boldsymbol{a}_i$'s, $\mathscr{E} \subset \mathbb{R}^{n_d}$ the basic strain subspace, $\mathscr{S}' \subset \mathbb{R}^{n_d}$ the basic stress subspace, and $\bar{\mathscr{S}} \subset \mathbb{R}^{n_d}$ the stress subspace by the mode $\bar{\boldsymbol{\sigma}}_j$'s of uni-axial stress or pure shear stress, in which $n_d = 3$, $m = 13$ and $\bar{M} = 18$ for 2D 8-node element. As discussed earlier, to find the optimal stress modes for hybrid element, the sub-modes have to be compared with their original basic modes using their similarity degrees. However, the similarity degree depends upon the inner product. It is well known for the energy product

$$\left\langle \boldsymbol{\varepsilon}_i, \boldsymbol{\sigma}_j \right\rangle = \int_{V^e} \boldsymbol{\varepsilon}_i^T \boldsymbol{\sigma}_j \, dV,\ \boldsymbol{\varepsilon}_i \in \mathscr{E}, \boldsymbol{\sigma}_j \in \mathscr{S} \qquad (17)$$

This is a conventional inner product where both the strain modes and stress modes are considered as mathematical vectors. However, the strain and stress belong to different mechanical concepts, and their analysis should be in mechanics for our attempt. In addition, even though the inner product has the physical meaning of energy, there is not any physical meaning in the associated norms or generalized lengths of strains and stresses as

$$\|\boldsymbol{\varepsilon}_i\| = \left(\int_{V^e} \boldsymbol{\varepsilon}_i^T \boldsymbol{\varepsilon}_i \, dV \right)^{1/2},\ \|\boldsymbol{\sigma}_j\| = \left(\int_{V^e} \boldsymbol{\sigma}_j^T \boldsymbol{\sigma}_j \, dV \right)^{1/2} \qquad (18)$$

In other words, the strain and stress are only considered as mathematical vectors without any physical meanings. Clearly, without appropriate norm and the relating inter angle, the comparison between the stress modes and basic strain modes is impossible. So, the further discussion is difficult, particularly for some stress modes of which the energy products with their related basic strain

modes are equal to each other. Therefore, the inappropriate energy product is found to be the big barrier to determine the optimal stress modes inside the basic stress field. To overcome this problem, the inner product with material matrix as weighting matrix is introduced as

$$\left\langle \boldsymbol{\sigma}_i', \mathbf{S}(\boldsymbol{\sigma}_i')_k \right\rangle = \int_{V^e} \boldsymbol{\sigma}_i'^T \mathbf{S}(\boldsymbol{\sigma}_i')_k dV, \ \boldsymbol{\sigma}_i', (\boldsymbol{\sigma}_i')_k \in \mathscr{S}' \cup \overline{\mathscr{S}} \tag{19}$$

The associated norms are expressed as

$$\left\| \boldsymbol{\sigma}_i' \right\|_S = \left(\int_{V^e} \boldsymbol{\sigma}_i'^T \mathbf{S} \boldsymbol{\sigma}_i' dV \right)^{1/2} = \left(\int_{V^e} \boldsymbol{\varepsilon}_i^T \mathbf{C} \boldsymbol{\varepsilon}_i dV \right)^{1/2}, \ \left\| (\boldsymbol{\sigma}_i')_k \right\|_S = \left(\int_{V^e} (\boldsymbol{\sigma}_i')_k^T \mathbf{S}(\boldsymbol{\sigma}_i')_k dV \right)^{1/2} \tag{20}$$

These norms have the specific physical significance as the flexibility of stress (or stiffness of strain), which is the square root of complementary energy (or deformation energy, in the case of linear elasticity they are equal to each other). It shows the relationship between two stress modes. So this inner product is more reasonable. For this sense, the inner product in Eq. (20) can be used for the quantitative analysis to calculate the similarity degree of the sub-modes with their basic stress mode. It should be noted that our inner product in Eq. (19) is the development from Zhang et al. (2002) where our inner product is defined in the mixed subspace of basic stress subspace $\mathscr{S}'$ together with $\overline{\mathscr{S}}$ in Eq. (16) rather than the assumed subspace $\mathscr{S}$ in Eq. (5). Based on our inner product in Eq. (19), the sub-modes can be compared with their basic stress modes to determine the optimal mode according to their similarity degrees.

Optimal stress field for 2D 8-node hybrid element

For the 2D 8-node quadrilateral hybrid element (HQ8) in Fig.1 where 5,6,7,8 are the mid nodes on the sides, there are $n = 16$ degrees of freedom including $r = 3$ rigid body motions and $m = n - r = 13$ deformations. The element displacement field in Eq. (6) can be written as

$$\begin{cases} u = A_0 + A_1 x + A_2 y + A_3 xy \\ \quad + A_4 x^2 + A_5 y^2 + A_6 x^2 y + A_7 xy^2 \\ v = B_0 + B_1 x + B_2 y + B_3 xy \\ \quad + B_4 x^2 + B_5 y^2 + B_6 x^2 y + B_7 xy^2 \end{cases} \tag{21}$$
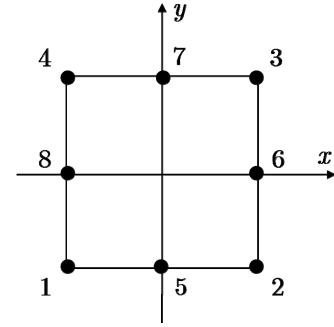
Fig.1 2D 8-node quadrilateral element

where $A_i, B_i, i = 0, 1, \cdots, 7$ are the coefficients dependent upon the nodal displacements. Thus the basic strains modes in Eq. (8) can be derived as

$$\bar{\boldsymbol{B}} = \begin{bmatrix} 1 & 0 & 0 & y & 2x & 2xy & y^2 & 0 & 0 & 0 & 0 & 0 & 0 \\ 0 & 1 & 0 & 0 & 0 & 0 & 0 & x & 2y & 2xy & x^2 & 0 & 0 \\ 0 & 0 & 2 & x & 0 & x^2 & 2xy & y & 0 & y^2 & 2xy & 2y & 2x \end{bmatrix} \tag{22}$$

In addition, the basic stress modes in Eq. (9) can be obtained as

$$\boldsymbol{P}' = \begin{bmatrix} C & \nu C & 0 & Cy & 2Cx & 2Cxy & Cy^2 & \nu Cx & 2\nu Cy & 2\nu Cxy & \nu Cx^2 & 0 & 0 \\ \nu C & C & 0 & \nu Cy & 2\nu Cx & 2\nu Cxy & \nu Cy^2 & Cx & 2Cy & 2Cxy & Cx^2 & 0 & 0 \\ 0 & 0 & 2G & Gx & 0 & Gx^2 & 2Gxy & Gy & 0 & Gy^2 & 2Gxy & 2Gy & 2Gx \end{bmatrix} \tag{23}$$

in which $C = E/(1-\nu^2)$, $G = E/(2(1+\nu))$ for Young's modulus E and Poison's ratio ν. To take away the unnecessary components inside the basic stress modes in Eq. (23), they are broken into sub-modes in Eq. (14) with $\bar{\boldsymbol{\sigma}}_j$'s expressed as

$$\bar{\boldsymbol{P}} = \{ \bar{\boldsymbol{\sigma}}_1, \bar{\boldsymbol{\sigma}}_2, \cdots, \bar{\boldsymbol{\sigma}}_{18} \} = \{ \boldsymbol{I}_3, x\boldsymbol{I}_3, y\boldsymbol{I}_3, xy\boldsymbol{I}_3, x^2\boldsymbol{I}_3, y^2\boldsymbol{I}_3 \} \tag{24}$$

in which $\boldsymbol{I}_3$ is the identity matrix of 3×3. Then sub-modes are compared with their original basic stress modes to select the optimal stress modes. The details are provided as follows:

5

(1) For σ_1', it can be broken into its sub-modes as

$$\begin{Bmatrix} C \\ \nu C \\ 0 \end{Bmatrix} = \begin{Bmatrix} C \\ 0 \\ 0 \end{Bmatrix} + \begin{Bmatrix} 0 \\ \nu C \\ 0 \end{Bmatrix} = C \begin{Bmatrix} 1 \\ 0 \\ 0 \end{Bmatrix} + \nu C \begin{Bmatrix} 0 \\ 1 \\ 0 \end{Bmatrix} \tag{25}$$

namely, $\sigma_1' = (\sigma_1')_1 + (\sigma_1')_2 = \bar{\alpha}_{11}\bar{\sigma}_1 + \bar{\alpha}_{12}\bar{\sigma}_2$, where $\bar{\alpha}_{11} = C$ and $\bar{\alpha}_{12} = \nu C$. Based on our inner product in Eq. (19) the following similarity degrees can be calculated as

$$\left| \cos \theta_{11} \right| = \frac{\sqrt{E}}{d_0}, \quad \left| \cos \theta_{12} \right| = 0 \tag{26}$$

where $d_0 = \sqrt{C}$. Since $\left| \cos \theta_{11} \right| > \left| \cos \theta_{12} \right|$, one can conclude that $(\sigma_1')_1$ is more similar than $(\sigma_1')_2$ with σ_1'. It indicates $(\sigma_1')_1$ represents more features than $(\sigma_1')_2$ inside σ_1'. Therefore, $\bar{\sigma}_1$ is selected as the optimal stress mode for hybrid element with respect to a_1 as $\sigma_1 = \bar{\sigma}_1$. The cases for σ_2', σ_5', and σ_9' are similar to σ_1' so that $\sigma_2 = \bar{\sigma}_2$, $\sigma_5 = \bar{\sigma}_4$, and $\sigma_9 = \bar{\sigma}_8$.

(2) For σ_3', since it is a pure shear stress mode as

$$\begin{Bmatrix} 0 \\ 0 \\ 2G \end{Bmatrix} = 2G \begin{Bmatrix} 0 \\ 0 \\ 1 \end{Bmatrix} \tag{27}$$

namely, $\sigma_3' = (\sigma_3')_3 = \bar{\alpha}_{33}\bar{\sigma}_3$, where $\bar{\alpha}_{33} = 2G$, the optimal stress mode is selected as $\sigma_3 = \bar{\sigma}_3$. The cases for σ_{12}', and σ_{13}' are similar to σ_3' so that $\sigma_{12} = \bar{\sigma}_9$ and $\sigma_{13} = \bar{\sigma}_6$.

(3) For σ_4', it can be broken into its sub-modes as

$$\begin{Bmatrix} Cy \\ \nu Cy \\ 2Gx \end{Bmatrix} = \begin{Bmatrix} Cy \\ 0 \\ 0 \end{Bmatrix} + \begin{Bmatrix} 0 \\ \nu Cy \\ 0 \end{Bmatrix} + \begin{Bmatrix} 0 \\ 0 \\ 2Gx \end{Bmatrix} = C \begin{Bmatrix} y \\ 0 \\ 0 \end{Bmatrix} + \nu C \begin{Bmatrix} 0 \\ y \\ 0 \end{Bmatrix} + 2G \begin{Bmatrix} 0 \\ 0 \\ x \end{Bmatrix} \tag{28}$$

namely, $\sigma_4' = (\sigma_4')_1 + (\sigma_4')_2 + (\sigma_4')_3 = \bar{\alpha}_{41}\bar{\sigma}_7 + \bar{\alpha}_{42}\bar{\sigma}_8 + \bar{\alpha}_{43}\bar{\sigma}_6$, where $\bar{\alpha}_{41} = C$, $\bar{\alpha}_{42} = \nu C$, and $\bar{\alpha}_{43} = 2G$. The following similarity degrees based on our inner product can be obtained as

$$\left| \cos \theta_{41} \right| = \frac{\sqrt{E}}{d_1}, \quad \left| \cos \theta_{42} \right| = 0, \quad \left| \cos \theta_{43} \right| = \frac{\sqrt{G}}{d_1} \tag{29}$$

where $d_1 = \sqrt{C+G}$. Due to the fact that the Poison's ratio in general satisfies $0 < \nu < 0.5$, one has $G < E$. Thus by Eq. (29) one can obtain $\left| \cos \theta_{41} \right| > \left| \cos \theta_{43} \right| > \left| \cos \theta_{42} \right|$. Then we find the expected optimal mode for a_4 as $\sigma_4 = \bar{\sigma}_7$. Obviously, by our systematic scheme, the parasitic shears $\tau_{xy} = Gx$ in σ_4' are taken away automatically. The case for σ_8' is similar to σ_4' so that $\sigma_8 = \bar{\sigma}_5$.

(4) For σ_6', it can be broken to its sub-modes as

$$\begin{Bmatrix} 2Cxy \\ 2\nu Cxy \\ Gx^2 \end{Bmatrix} = \begin{Bmatrix} 2Cxy \\ 0 \\ 0 \end{Bmatrix} + \begin{Bmatrix} 0 \\ 2\nu Cxy \\ 0 \end{Bmatrix} + \begin{Bmatrix} 0 \\ 0 \\ Gx^2 \end{Bmatrix} = 2C \begin{Bmatrix} xy \\ 0 \\ 0 \end{Bmatrix} + 2\nu C \begin{Bmatrix} 0 \\ xy \\ 0 \end{Bmatrix} + G \begin{Bmatrix} 0 \\ 0 \\ x^2 \end{Bmatrix} \tag{30}$$

namely, $\sigma_6' = (\sigma_6')_1 + (\sigma_6')_2 + (\sigma_6')_3 = \bar{\alpha}_{61}\bar{\sigma}_{10} + \bar{\alpha}_{62}\bar{\sigma}_{11} + \bar{\alpha}_{63}\bar{\sigma}_{15}$, where $\bar{\alpha}_{61} = 2C$, $\bar{\alpha}_{62} = 2\nu C$, and $\bar{\alpha}_{63} = G$. The following similarity degrees based on our inner product can be obtained as

$$\left|\cos\theta_{61}\right|=\frac{4\sqrt{E}}{3d_2}, \ \left|\cos\theta_{62}\right|=0, \ \left|\cos\theta_{63}\right|=\frac{2\sqrt{5G}}{5d_2} \tag{31}$$

where $d_2=\sqrt{4G/5+16C/9}$. Since $0<\nu<0.5$, one has $\left|\cos\theta_{61}\right|/\left|\cos\theta_{63}\right|=2\sqrt{10(1+\nu)}/3>1$. Thus $\left|\cos\theta_{61}\right|>\left|\cos\theta_{63}\right|>\left|\cos\theta_{62}\right|$. Then the expected optimal mode can be determined as $\boldsymbol{\sigma}_6=\overline{\boldsymbol{\sigma}}_{10}$. The case for $\boldsymbol{\sigma}'_{10}$ is similar to $\boldsymbol{\sigma}'_6$ so that $\boldsymbol{\sigma}_{10}=\overline{\boldsymbol{\sigma}}_{11}$.

(5) For $\boldsymbol{\sigma}'_7$, it can be broken to its sub-modes as

$$\begin{Bmatrix} Cy^2 \\ \nu Cy^2 \\ 2Gxy \end{Bmatrix}=\begin{Bmatrix} Cy^2 \\ 0 \\ 0 \end{Bmatrix}+\begin{Bmatrix} 0 \\ \nu Cy^2 \\ 0 \end{Bmatrix}+\begin{Bmatrix} 0 \\ 0 \\ 2Gxy \end{Bmatrix}=C\begin{Bmatrix} y^2 \\ 0 \\ 0 \end{Bmatrix}+\nu C\begin{Bmatrix} 0 \\ y^2 \\ 0 \end{Bmatrix}+2G\begin{Bmatrix} 0 \\ 0 \\ xy \end{Bmatrix} \tag{32}$$

namely, $\boldsymbol{\sigma}'_7=(\boldsymbol{\sigma}'_7)_1+(\boldsymbol{\sigma}'_7)_2+(\boldsymbol{\sigma}'_7)_3=\overline{\alpha}_{71}\overline{\boldsymbol{\sigma}}_{16}+\overline{\alpha}_{72}\overline{\boldsymbol{\sigma}}_{17}+\overline{\alpha}_{73}\overline{\boldsymbol{\sigma}}_{12}$, where $\overline{\alpha}_{71}=C$, $\overline{\alpha}_{72}=\nu C$, and $\overline{\alpha}_{73}=2G$. The following similarity degrees can be obtained as

$$\left|\cos\theta_{71}\right|=\frac{2\sqrt{5E}}{5d_2}, \ \left|\cos\theta_{72}\right|=0, \ \left|\cos\theta_{73}\right|=\frac{4\sqrt{G}}{3d_2} \tag{33}$$

Since $\left|\cos\theta_{71}\right|/\left|\cos\theta_{73}\right|=\sqrt{9(1+\nu)/10}$, one can conclude $\cos\theta_{71}>\cos\theta_{73}$ when $\nu>1/9$ which is the case for most materials. Then the expected optimal mode can be selected as $\boldsymbol{\sigma}_7=\overline{\boldsymbol{\sigma}}_{16}$. The case for $\boldsymbol{\sigma}'_{11}$ is similar to $\boldsymbol{\sigma}'_7$ so that $\boldsymbol{\sigma}_{11}=\overline{\boldsymbol{\sigma}}_{14}$.

In summary, the final optimal stress modes are expressed as

$$\begin{aligned}
\boldsymbol{P}&=\{\boldsymbol{\sigma}_1,\cdots,\boldsymbol{\sigma}_{13}\}=\{\overline{\boldsymbol{\sigma}}_1,\overline{\boldsymbol{\sigma}}_2,\overline{\boldsymbol{\sigma}}_3,\overline{\boldsymbol{\sigma}}_7,\overline{\boldsymbol{\sigma}}_4,\overline{\boldsymbol{\sigma}}_{10},\overline{\boldsymbol{\sigma}}_{16},\overline{\boldsymbol{\sigma}}_5,\overline{\boldsymbol{\sigma}}_8,\overline{\boldsymbol{\sigma}}_{11},\overline{\boldsymbol{\sigma}}_{14},\overline{\boldsymbol{\sigma}}_9,\overline{\boldsymbol{\sigma}}_6\} \\
&=\begin{bmatrix} 1 & 0 & 0 & y & x & xy & y^2 & 0 & 0 & 0 & 0 & 0 & 0 \\ 0 & 1 & 0 & 0 & 0 & 0 & 0 & x & y & xy & x^2 & 0 & 0 \\ 0 & 0 & 1 & 0 & 0 & 0 & 0 & 0 & 0 & 0 & 0 & y & x \end{bmatrix}
\end{aligned} \tag{34}$$

Using the method by Zhang and Wang (2006, 2010), it is easy to verify that the element HQ8 constructed by the optimal stress modes in Eq. (34) is free of zero-energy mode.

Numerical example
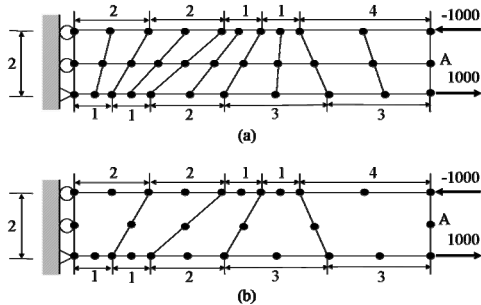

Fig 2. Cantilever beam (a) Q4 (b) Q8

Table 1 Tip deflections v_A for cantilever beams

ν	0.25	0.49	0.499	0.4999
Q4	69.30	18.22	5.71157	2.713
Q8	93.34	73.79	65.3585	46.366
HQ4	93.23	75.20	74.2974	74.206
HQ8	93.72	75.49	74.5796	74.488
Exact	93.75	75.99	75.0999	75.010

A simple test for volume locking is given in Fig 2. This is an elastic plane-strain cantilever beam for $E=1500$ and different Poison's ratio ν. It is simply supported and subjected to pure bending. The results are provided in Table 1. It is shown that, when ν tends to 0.5, the solution for improper elements show volumetric locking while HQ8 yields the most accurate solution for the tip deflection v_A. So the present element can overcome the volumetric locking successfully.

7

Conclusions

A new inner product with the material matrix as the weighting matrix was introduced to study the relationship quantitatively between the different stress modes. Besides, the basic stress modes are considered instead of the basic strain modes in the conventional hybrid finite element formulation. They are broken into a set of sub-modes and these sub-modes are compared with their original basic stress modes to construct the optimal stress field for 2D 8-node quadrilateral hybrid element. The proposed method is straightforward to investigate the basic stress modes and determine the optimal stress modes, while the methods based on the conventional energy product as well as the modal technique can only be used to select the zero energy free stress modes.

Acknowledgements

References

Bilotta, A. and Casciaro, R. (2002), Assumed stress formulation of high order quadrilateral elements with an improved in-plane bending behaviour, *Computer Methods in Applied Mechanics and Engineering*, 191, pp, 1523-1540.

Cen, S., Zhou, M. J. and Fu, X. R. (2011), A 4-node hybrid stress-function (HS-F) plane element with drilling degrees of freedom less sensitive to severe mesh distortions. *Computers & Structures*, 89, pp, 517-528.

Feng, W. and Hoa, S. V. and Huang, Q. (1997), Classification of stress modes in assumed stress fields of hybrid finite elements. *International Journal for Numerical Methods in Engineering*, 40, pp, 4313-4339.

Han, J. and Hoa, S. V. (1993), A three-dimensional multilayer composite finite element for stress analysis of composite laminates. *International Journal for Numerical Methods in Engineering*, 36, pp, 3903-3914.

Huang, Q. (1991), Modal analysis of deformable bodies with finite degree of deformation freedom-an approach to determination of natural stress modes in hybrid finite elements. In: Chien WZ, Fu ZZ, eds. *Advances in Applied Mathematics & Mechanics in China*, IAP, 3, pp. 283-303.

Pian, T. H. H. (1964), Derivation of element stiffness matrices. *AIAA Journal*; 2, pp. 576-577.

Pian, T. H. H. and Chen D. P. (1983), On the suppression of zero energy deformation modes. *International Journal for Numerical Methods in Engineering*, 19, pp. 1741-1752.

Pian, T. H. H. and Sumihara, K. (1984), Rational approach for assumed stress finite elements, *International Journal for Numerical Methods in Engineering*, 20, pp. 1685-1695.

Sze, Y. K. (1996), Admissible matrix formulation-from orthogonal approach to explicit hybrid stabilization, *Finite Elements in Analysis and Design*, 24, pp, 1-30.

Wu, C. C. and Cheung, Y. K. (1995), On optimization approaches of hybrid stress elements, *Finite Elements in Analysis and Design*, 21, pp, 111-128.

Zhang, C., Feng, W. and Huang, Q. (2002), The stress subspace of hybrid stress element and the diagonalization method for flexibility matrix H, *Applied Mathematics and Mechanics*, 23, pp. 1263-1273.

Zhang, C., Huang. Q. and Feng, W. (2006), Deformation rigidity of assumed stress modes in hybrid elements. *Applied Mathematics and Mechanics*, 27, pp. 861-869.

Zhang C. and Wang, D. (2006), Suppression of zero-energy modes in hybrid finite elements via assumed stress fields, *EPMESC-X*, pp, 21-23.

Zhang, C., Wang, D., Zhang, J., Feng, W. and Huang, Q. (2007), On the equivalence of various hybrid finite elements and a new orthogonalization method for explicit element stiffness formulation. *Finite Elements in Analysis and Design*, 2007; 43, pp. 321-332.

Zhang, C, and Wang, D. (2010), An assumed stress method for zero-energy mode suppression in hybrid finite elements. *Chinese Journal of Solid Mechanics*, 31, pp. 40-47.

Zhang, C., Wang, D. and Li, T. (2011b), Orthogonal basic deformation mode method for zero-energy mode suppression of hybrid stress elements. *Applied Mathematics and Mechanics (English Edition)*, 32, pp. 83-96.